Short Article

Cell Metabolism

iNKT Cells Induce FGF21 for Thermogenesis and Are Required for Maximal Weight Loss in GLP1 Therapy

Graphical Abstract

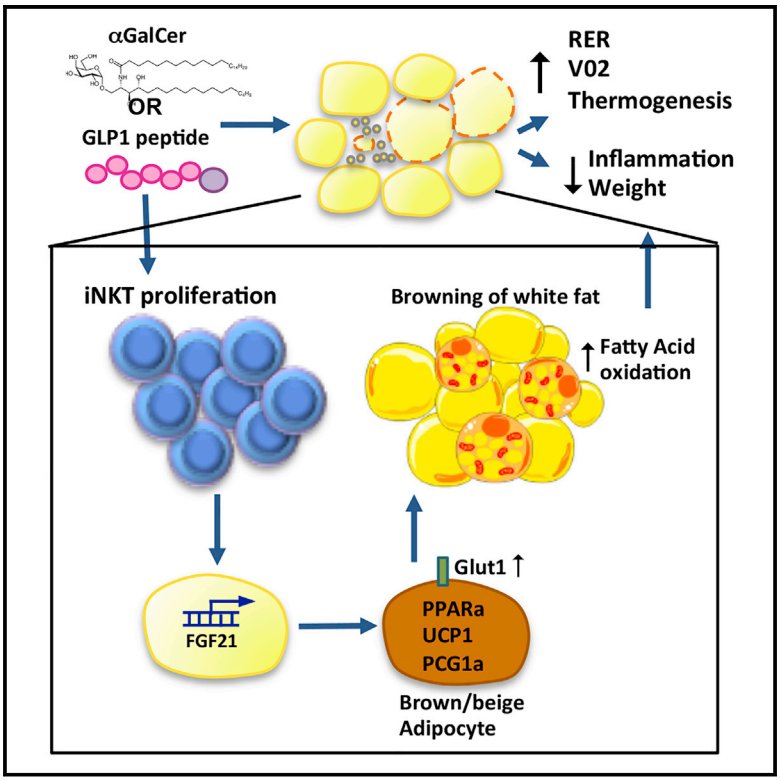

Highlights

- iNKT cell activation leads to potent weight loss and glycemic control in obesity
- iNKT-induced weight loss is induced by thermogenic browning of white fat
- FGF21 induced by iNKT cells plays an important step in weight loss
- GLP-1 activates iNKT cells, triggering FGF21 and contributing to weight loss

Authors

Lydia Lynch, Andrew E. Hogan, Danielle Duquette, ..., Daniel J. Drucker, Donal O'Shea, Michael Brenner

Correspondence

llynch@bwh.harvard.edu (L.L.), info@dosheaendo.ie (D.O.), mbrenner@research.bwh.harvard.edu (M.B.)

In Brief

Activation of adipose-resident invariant natural killer (iNKT) cells induces weight loss and restores glycemic control in obesity. Lynch et al. investigate the underlying mechanism and unveil a pathway involving FGF21. GLP-1 therapy also activated the iNKT-FGF21 axis, which contributes to weight loss.

Lynch et al., 2016, Cell Metabolism *24*, 1–10
September 13, 2016
http://dx.doi.org/10.1016/j.cmet.2016.08.003

CellPress

Please cite this article in press as: Lynch et al., iNKT Cells Induce FGF21 for Thermogenesis and Are Required for Maximal Weight Loss in GLP1 Therapy, Cell Metabolism (2016), http://dx.doi.org/10.1016/j.cmet.2016.08.003

Cell Metabolism
Short Article

CellPress

iNKT Cells Induce FGF21 for Thermogenesis and Are Required for Maximal Weight Loss in GLP1 Therapy

Lydia Lynch,[1,2,8,*] Andrew E. Hogan,[3] Danielle Duquette,[1] Chantel Lester,[1] Alexander Banks,[2] Katherine LeClair,[4] David E. Cohen,[4] Abhisek Ghosh,[1] Bing Lu,[1] Michelle Corrigan,[3] Darko Stevanovic,[5] Eleftheria Maratos-Flier,[5] Daniel J. Drucker,[6] Donal O'Shea,[3,7,*] and Michael Brenner[1,*]

[1]Division of Rheumatology, Immunology, and Allergy, Department of Medicine
[2]Division of Endocrinology
Brigham and Women's Hospital, Harvard Medical School, Boston, MA 02115, USA
[3]Education and Research Center and Conway Institute, St. Vincent's University Hospital, University College Dublin, Dublin 4, Ireland
[4]Division of Gastroenterology, Department of Medicine, Brigham and Women's Hosital, Harvard Medical School, Boston, MA 02115, USA
[5]Division of Endocrinology, Beth Israel Deaconess Medical Center, Boston, MA 02215, USA
[6]The Lunenfeld-Tanenbaum Research Institute, Mount Sinai Hospital, University of Toronto, Toronto, ON M5G 1X5, Canada
[7]Department of Endocrinology, St. Vincent's University Hospital, University College Dublin, Dublin 4, Ireland
[8]Lead Contact
*Correspondence: llynch@bwh.harvard.edu (L.L.), info@dosheaendo.ie (D.O.), mbrenner@research.bwh.harvard.edu (M.B.)
http://dx.doi.org/10.1016/j.cmet.2016.08.003

SUMMARY

Adipose-resident invariant natural killer T (iNKT) cells are key players in metabolic regulation. iNKT cells are innate lipid sensors, and their activation, using their prototypic ligand α-galactosylceramide (αGalCer), induces weight loss and restores glycemic control in obesity. Here, iNKT activation induced fibroblast growth factor 21 (FGF21) production and thermogenic browning of white fat. Complete metabolic analysis revealed that iNKT cell activation induced increased body temperature, V02, VC02, and fatty acid oxidation, without affecting food intake or activity. FGF21 induction played a major role in iNKT cell-induced weight loss, as FGF21 null mice lost significantly less weight after αGalCer treatment. The glucagon-like peptide 1 (GLP-1) receptor agonist, liraglutide, also activated iNKT cells in humans and mice. In iNKT-deficient mice, liraglutide promoted satiety but failed to induce FGF21, resulting in less weight loss. These findings reveal an iNKT cell-FGF21 axis that defines a new immune-mediated pathway that could be targeted for glycemic control and weight regulation.

INTRODUCTION

Obesity threatens to shorten the human lifespan by 5–20 years, the biggest burden being obesity-induced diseases (Wang et al., 2011). Obesity is far more complex and touches many more aspects of biology than was previously appreciated. Currently, therapy for obesity is limited by an incomplete understanding of how body weight is controlled. A promising potential approach for treating obesity is activation of brown adipose tissue (BAT). In contrast to energy-storing white adipose tissue (WAT), BAT contains many thermogenic mitochondria that express uncoupling protein 1 (UCP-1), which dissipates chemical energy into heat (Enerbäck et al., 1997). Recently, it was shown that multi-locular adipocytes expressing UCP-1 can also be induced in WAT, known as beige or brite cells (Cousin et al., 1992; Enerbäck, 2009). Browning of WAT uses large amounts of energy through induction of β-oxidation, resulting in increased metabolic rate and weight loss. Chronic cold exposure and β-adrenergic stimulation are physiological inducers of browning in WAT (Cousin et al., 1992; Himms-Hagen et al., 1994). More recently, the hormone fibroblast growth factor 21 (FGF21), produced in liver, WAT, and BAT, was shown to improve metabolic disease and induce weight loss in humans and mice (Gaich et al., 2013; Hanssen et al., 2015; Kharitonenkov and Adams, 2013; Kharitonenkov et al., 2005; Samms et al., 2015). Recently, a synthetic FGF21 variant, LY2405319, was shown to reduce low-density lipoprotein (LDL) cholesterol and triglycerides, increase adiponectin levels, improve fasting insulin, and induce weight loss in obese patients with type 2 diabetes (Gaich et al., 2013). FGF21 administration has been associated with increased UCP-1 levels, which are required for FGF21-induced thermogenesis; however, FGF21 reduces food intake, contributing to weight loss, independently of UCP-1 (Samms et al., 2015). These studies position FGF21 as a promising drug target for the treatment of metabolic disorders.

Recent studies have highlighted a role for the innate immune system in activation of BAT and induction of browning in WAT. Alternatively activated macrophages can produce catecholamines in response to cold exposure, which activates BAT and induces lipolysis in WAT (Nguyen et al., 2011). Eosinophils, which secrete IL-4 and IL-13, sustain alternative macrophage activation and catecholamine production in cold settings (Qiu et al., 2014). Independent of cold exposure, cytokines including IL-33 are critical for maintaining innate lymphoid cells (ILCs) in adipose tissue, which are key players in regulating energy expenditure (Molofsky et al., 2013). ILCs can also induce browning by producing methionine-enkephalin, which upregulates UCP1^{+} beige

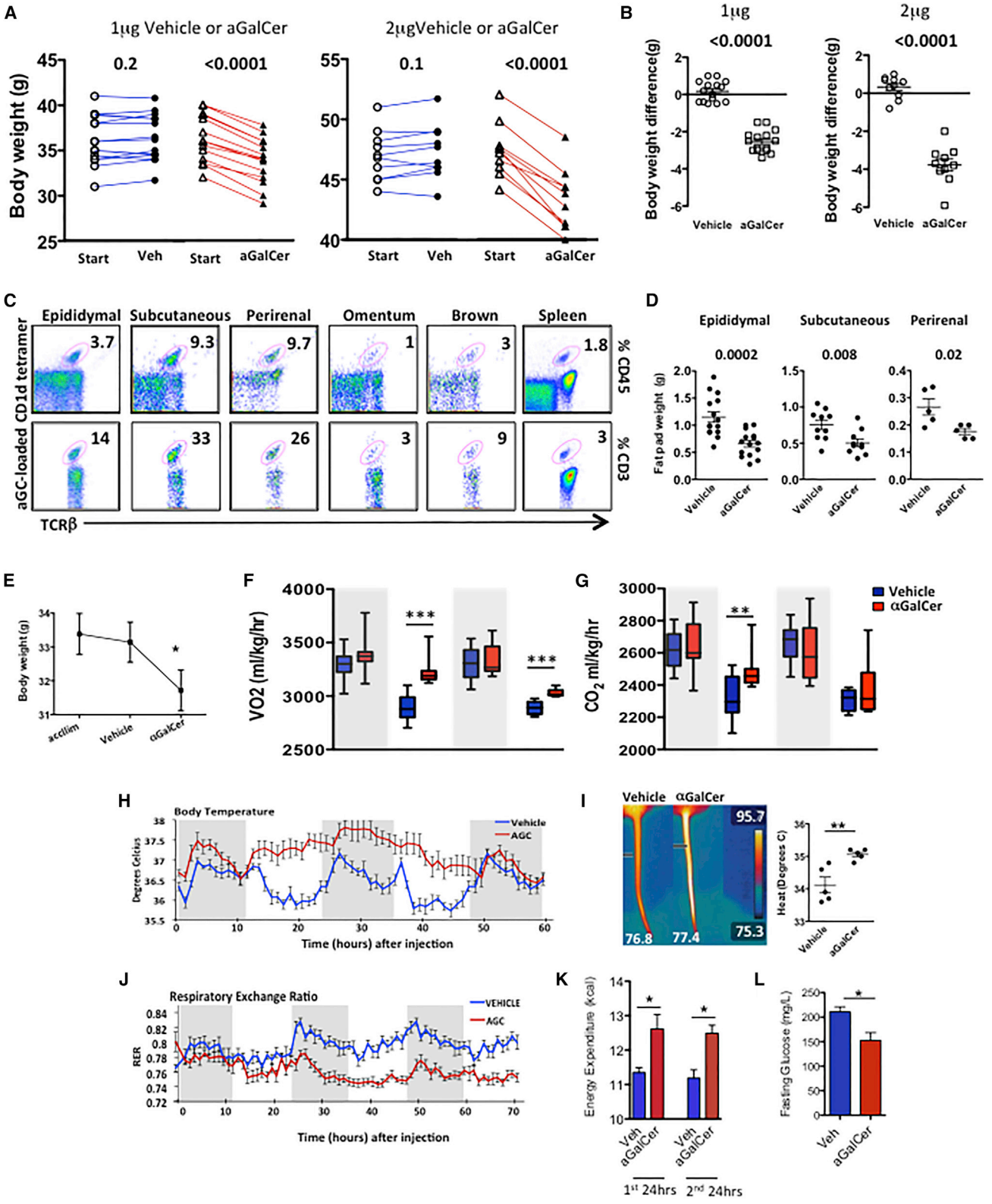

Figure 1. Activation of iNKT Cells Induces Weight Loss through Thermogenesis

(A) Body weight of obese WT mice 4 days after one injection of 1 μg/mouse (n = 15 per group) (left) or 2 μg/mouse (n = 10 per group) (right) αGalCer or vehicle control.

(B) Change in body weight after αGalCer or vehicle control.

(legend continued on next page)

adipocytes in WAT (Brestoff et al., 2015). Thus, recent studies have solidified the role of the adipose innate immune system in the regulation of metabolism and body weight.

Invariant natural killer T (iNKT) cells are one such innate immune cell type with an important role in weight and glycemic control. iNKT cells are activated by lipid antigens presented by CD1d molecules (Brigl and Brenner, 2004). We and others have shown that iNKT cells are enriched in human and murine adipose tissue (Lynch et al., 2009, 2012), and that iNKT cells can regulate body weight and restore metabolic homeostasis in obesity (Hams et al., 2013; Huh et al., 2013; Ji et al., 2012; Lynch et al., 2012; Schipper et al., 2012). Recently, we found that adipose iNKT cells are a unique regulatory subset of iNKT cells with a distinct gene expression profile and anti-inflammatory functions (Lynch et al., 2015). Adipose iNKT cells are reduced in obesity, but activating iNKT cells with their prototypical lipid ligand α-galactosylceramide (αGalCer) causes their expansion, which induces potent weight loss; however, the weight loss mechanism is not understood. Here, we report that iNKT cell-induced weight loss occurs through browning of WAT and thermogenesis, without loss of appetite. Furthermore, FGF21 induction is a key player in this weight loss pathway. This iNKT-FGF21 pathway plays a physiological role in a subset of the actions of glucagon-like peptide 1 (GLP-1), a gut hormone that controls glycemia and satiety (Turton et al., 1996), leading to weight loss (Baggio and Drucker, 2007). In rodents, GLP-1 also regulates body temperature (O'Shea et al., 1996) and activates pathways associated with increased numbers of thermogenic beige and brown adipocytes (Lockie et al., 2012). Here, we show that murine iNKT cells contribute to the weight loss effects observed with administration of GLP-1 receptor (GLP-1R) agonists.

RESULTS AND DISCUSSION

To investigate the mechanism of iNKT cell-induced weight loss, we specifically activated iNKT cells in obese mice by using their lipid antigen ligand αGalCer. A single intraperitoneal (i.p.) injection of αGalCer potently induced weight loss in obese mice (Figures 1A and 1B). The effects of αGalCer were dose dependent; 1 μg αGalCer induced an average of 2.5 g of body weight in obese mice on high-fat diet (HFD) for 6–12 weeks (n = 15) (Figures 1A and 1B; $p \leq 0.0001$), while mice fed an HFD of longer duration (16–20 weeks) received 2 μg αGalCer and lost significantly more body weight (3.7 g lost with αGalCer, n = 10; versus 0.3 g increase with vehicle control, n = 10). We have previously shown that αGalCer reduces the percentage of fat mass, but not lean mass, in mice as measured by dual X-ray absorptiometry (DEXA) (Lynch et al., 2012). The reduction in total body fat after αGalCer prompted us to look at other fat depots in addition to epididymal fat pads. We found that iNKT cells are enriched in all adipose depots examined compared to spleen, except omentum, which contained fewer iNKT cells (Figure 1C). αGalCer activated iNKT cells in all adipose depots (as measured by iNKT cell expansion >3-fold and CD69 upregulation; data not shown) and induced a significant decrease in fat pad mass in the epididymal, subcutaneous, and perirenal adipose depots (Figure 1D). Thus, specific αGalCer activation of iNKT cells induces potent body weight loss associated with a reduction in the fat mass of several fat depots.

To understand how iNKT cell activation induces a rapid reduction of ~10% of body weight in 4 days, we measured whole-body metabolism using Complete Lab Animal Monitoring System (CLAMS). Obese mice (n = 6) were placed in the CLAMS and served as their own controls: they were first acclimatized and then received vehicle control (1 μg), metabolic readouts were measured for 70 hr, and then they received 1 μg αGalCer treatment and remained in the chambers for 70 hr. As before, mice lost significant weight after αGalCer treatment, but not vehicle control. Unlike control-treated mice, a single αGalCer injection induced an increase in VO_2 and VCO_2 (Figures 1F and 1G). There was a slight, but not significant, reduction in locomotor activity after αGalCer treatment, and despite weight loss, there was no reduction in daily food intake (Figures S1A and S1B, available online). αGalCer treatment induced a robust and consistent increase in thermogenesis (Figure 1H). To confirm this increase in thermogenesis, we performed a separate experiment where obese mice received vehicle (n = 5) or αGalCer (n = 5), and body temperature was visualized using a forward-looking infrared (FLIR) camera, showing that αGalCer treatment induced a 1° rise in body temperature (Figure 1I). Most strikingly, αGalCer induced a significant decrease in the respiratory exchange ratio (RER) (Figure 1J), which is a measurement of substrate utilization. Decreased RER shows preferential burning of fat, rather than carbohydrates, as the main source of energy, indicating induction of β-oxidation. After adjusting for food

(C) Flow plots of iNKT cells, measured by αGalCer-loaded CD1d tetramer+ cells in various adipose depots and spleen, representing five individual mice. Numbers show percent of $CD45^+$ cells (top) and percent of T cells (bottom).
(D) Change in epididymal (n = 15 per group), subcutaneous (n = 10 per group), and perirenal (n = 5 per group) fat pad size in obese WT mice 4 days post-αGalCer treatment.
(E) Body weight of obese WT mice 3 days after one injection of vehicle and then 3 days after 1 μg αGalCer, following CLAMS experiment (n = 6 per treatment).
(F and G) (F) O_2 consumption and (G) CO_2 production in obese WT mice acclimatized in metabolic cages, then treated with vehicle for 3 days, and then αGalCer for 3 days. Each mouse served as its own control (n = 6). Results displayed in 12 hr periods (shaded area represents the dark cycle).
(H) Body temperature measured by implanted peritoneal temperature probes.
(I) Infrared images and graph showing body temperature of obese WT mice 48 hr after receiving αGalCer (1 μg) or vehicle (n = 5 per treatment).
(J) RER of obese WT mice treated with vehicle control for 3 days (blue) or αGalCer for 3 days (red).
(K) Calculation of energy expenditure in the first and second 24 hr period following treatment with vehicle or αGalCer after adjustment for food intake and body weight.
In (J) and (K), n = 6 per group.
(L) Fasting blood glucose 4 days post-vehicle or 1 μg αGalCer treatment (n = 5–6 per group, two independent experiments). Small horizontal bars indicate the mean (± SEM).
Statistics have been calculated using a Student's paired t test (A and E) and unpaired t test (B, D, I, K, and L). *$p < 0.05$, **$p < 0.01$, ***$p < 0.001$.

intake and body weight of each mouse, energy expenditure calculations showed that one αGalCer treatment induced significantly higher energy expenditure in mice in each 24 hr period following treatment (Figure 1K). In addition to the weight loss, we confirmed our previous finding (Lynch et al., 2012) that αGalCer activation of iNKT cells in obese mice also improves fasting glucose levels (Figure 1L). This striking change in metabolic rate and energy homeostasis would explain the potent effects on weight loss seen with αGalCer treatment.

The induction of β-oxidation, thermogenesis, and reduced WAT suggested that activation of browning of WAT may have occurred. Consistent with this possibility, we found significant induction of $UCP1^{+}$ cells in inguinal WAT within 24 hr after αGalCer (Figure 2A). Cold temperatures and β-adrenergic stimulators are physiological activators of browning in WAT. As mice treated with αGalCer were housed at room temperature where full BAT activation is not required, we investigated iNKT-dependent mechanisms leading to browning of WAT. FGF21 has been shown to improve metabolic disorders and induce weight loss in humans and mice (Kharitonenkov and Adams, 2013). FGF21 has been implicated in inducing a thermogenic program in WAT through activation of PGC1α (Fisher et al., 2012), as well as by induction of adiponectin, leading to increased energy expenditure (Holland et al., 2013). Administration of αGalCer strongly induced FGF21 transcripts in inguinal adipose tissue within 3 hr of administration, to a similar extent as the β3-adrenoreceptor agonist CL316,243 (Figure 2B). At 3 hr after αGalCer, FGF21 was not activated in BAT; however, by 24 hr after αGalCer treatment, FGF21 transcripts were also significantly induced in BAT and further increased in inguinal adipose tissue (Figures 2B and 2C). In contrast, FGF21 expression was not induced in WAT or BAT of $CD1d^{-/-}$ (iNKT deficient) mice after αGalCer, confirming an iNKT-dependent effect (Figure 2C). FGF21 protein secretion was also significantly increased from explants of inguinal WAT and BAT after αGalCer treatment (Figure 2D). Furthermore, serum FGF21 levels were significantly elevated after αGalCer treatment, at even higher levels than those detected after administration of CL316,243 (Figure 2E). Surprisingly, despite the liver being another key source of iNKT cells and FGF21, αGalCer treatment did not increase FGF21 levels in liver (Figure S1C). αGalCer also induced adiponectin in inguinal adipose tissue of wild-type (WT), but not in $CD1d^{-/-}$, mice (Figure 2F). Although αGalCer is a specific activator of iNKT cells and is not a β-adrenoreceptor agonist, we assessed if iNKT cells could induce FGF21 without αGalCer activation. To examine this, we adoptively transferred iNKT cells into obese $CD1d^{-/-}$ mice (in vivo), and in another experiment, we co-cultured iNKT cells with obese adipose tissue (in vitro). In both types of experiments, iNKT cells increased levels of FGF21 protein, and adiponectin in adipose tissue (Figure 2G). Thus, our data show that iNKT activation or adoptive transfer induces FGF21, thermogenesis, and weight loss, implicating FGF21 as an important mediator of this pathway. To examine if FGF21 was required for iNKT-mediated weight loss, we investigated FGF21 null mice. $FGF21^{-/-}$ mice were fed an HFD for 12 weeks and treated with αGalCer or vehicle control. In the absence of FGF21, αGalCer-induced weight loss was significantly attenuated, compared to WT controls (Figure 2H). There was no statistical difference in the mean weight of the epididymal fat pads between groups (Figure 2I). Thus, iNKT cell activation or adoptive transfer induces FGF21, adiponectin, β-oxidation, browning of WAT, and increased energy expenditure leading to weight loss, which is partly dependent on induction of FGF21.

Discovery of an iNKT-FGF21 thermogenic pathway led us to question if this pathway was physiologically relevant in other weight loss settings. As we have previously shown that liraglutide and native GLP-1 can activate human iNKT cells (Hogan et al., 2011), and GLP-1 receptor signaling can regulate lymphocyte maintenance and proliferation (Hadjiyanni et al., 2010), we examined whether GLP-1R signaling-induced weight loss was dependent in part on iNKT cell activation. Obese mice fed an HFD for 8 weeks were treated with the GLP-1R agonist liraglutide or PBS control by i.p. injection daily for 5 days. As expected, liraglutide treatment lowered fasting glucose, improved glucose handling (Figure S2A), reduced body weight and epididymal fat pad weight (Figures S2B and S2C), and decreased adipocyte size (Figure S2D). Consistent with our previous finding in humans, liraglutide increased iNKT cell frequency in blood and adipose tissue (Figures 3A and 3B). Adipose iNKT cells were activated by liraglutide treatment, evidenced by an increased expression of the activation marker CD69 in vivo (Figure 3C). Liraglutide also led to proliferation of adipose iNKT cells (Figure S2E) and increased their IL-10 production in vivo (Figure 3D), a hallmark of adipose iNKT cell regulatory function (Lynch et al., 2015). Furthermore, when tested in vitro, liraglutide directly induced proliferation in murine iNKT cell primary lines (Figure S2F) and induced their IL-10 production (Figures S2G and S2H). These results show that the GLP-1 analog liraglutide can activate iNKT cells in vivo and directly in vitro.

As liraglutide activates iNKT cells, and both liraglutide (Lovshin and Drucker, 2009) and iNKT cell activation can promote weight loss (Lynch et al., 2012), we determined whether GLP-1-iNKT cell interactions were relevant to the metabolic and weight loss effects of liraglutide GLP-1-based therapy. We fed WT and $CD1d^{-/-}$ mice (lacking iNKT cells) an HFD for 8 weeks and treated them with liraglutide. The absence of iNKT cells did not impact the glycemic effects of liraglutide (Figures 3E and 3F), for liraglutide induces similar reductions in fasting glucose and glycemic excursion in both WT and $CD1d^{-/-}$ mice. However, the presence of iNKT cells was required for the full weight loss effects after several days of liraglutide administration; $CD1d^{-/-}$ mice lost approximately one-third less overall weight than WT mice after liraglutide treatment (Figure 3G). Although liraglutide produced a significant reduction in food intake in both WT and $CD1d^{-/-}$ (Figure S2I), $CD1d^{-/-}$ mice regained their weight and exhibited no weight loss between days 2 and 6 following liraglutide treatment, unlike WT mice, which continued to lose weight (Figures 3H and 3I). Similar findings (less weight loss with liraglutide) were seen in $Ja18^{-/-}$ mice on HFD, a second murine model that lacks iNKT cells due to deletion of the invariant Ja18 T cell receptor chain (Figure S3). $Ja18^{-/-}$ mice and WT mice lost similar weight in the first 24 hr, when food intake is severely reduced, but following this initial 24 hr period, WT continued to lose weight while $Ja18^{-/-}$ gained weight (Figures S3B–S3D). To rule out a central defect in GLP-1R signaling as a mechanism for resistance to liraglutide-induced weight loss, we found that *GLP1r* expression in the hypothalamus was similar in WT and

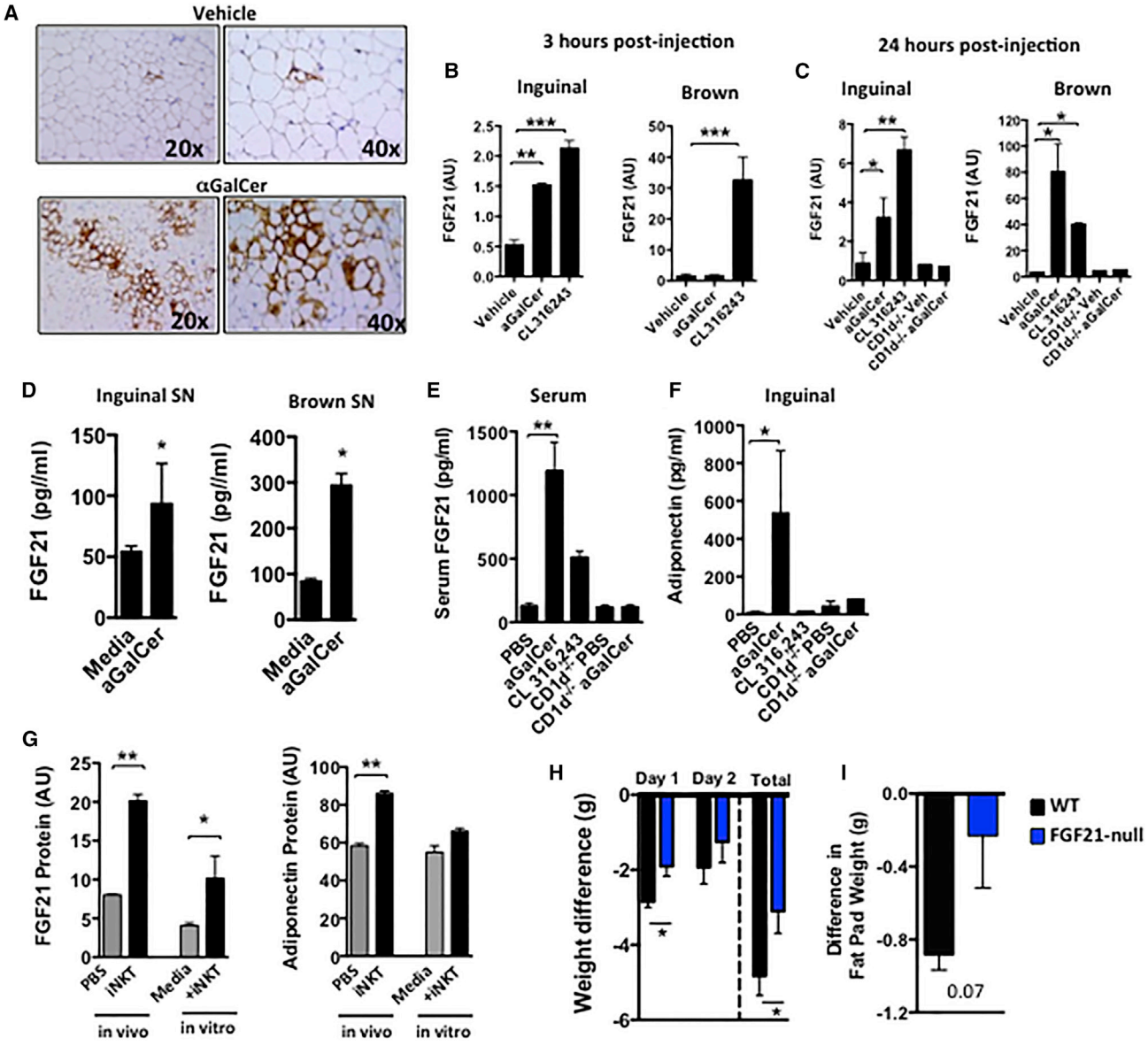

Figure 2. Activation of iNKT Cells Induces Browning of WAT, Partially through Induction of FGF21

(A) Immunohistochemical staining of UCP-1 protein in inguinal adipose tissue after vehicle control or αGalCer injection (representing one experiment with n = 4 per group, repeated twice).

(B and C) qPCR for FGF21 transcript in inguinal adipose tissue and brown adipose tissue (BAT) at (B) 3 hr or (C) 24 hr after vehicle (n = 7) or αGalCer treatment (n = 7), compared to β-adrenergic receptor agonist CL316,243 (1 mg/kg intraperitoneally) (n = 4) as a positive control (AU, arbitrary units).

(D) FGF21 protein level in supernatant of cultured ex vivo inguinal and brown adipose tissue, measured by ELISA, from mice treated in vivo with vehicle control or αGalCer (n = 5 per group).

(E) Serum concentration of FGF21 after αGalCer or CL316,243, in WT and *CD1d*$^{-/-}$ mice measured by ELISA (n = 5 per group).

(F) Adiponectin protein in inguinal adipose tissue after αGalCer or CL316,243, in WT and *CD1d*$^{-/-}$ mice measured by ELISA (n = 3 per group, repeated twice).

(G) WT obese mice received iNKT cell adoptive transfer intraperitoneally, and 2 days later, adipose tissue was cultured overnight. In another experiment, obese adipose tissue was co-cultured with isolated adipose iNKT cells (in vitro). Supernatant was collected from both experiments, and FGF21 and adiponectin proteins were measured (n = 4–5 per group).

(H and I) (H) Body weights and (I) epididymal fat pad weight of HFD-fed *FGF21*$^{-/-}$ mice (n = 6) and WT mice (n = 6) 3 days after one i.p. injection of 2 μg αGalCer or vehicle. Graphs show the mean (± SEM).

Statistics have been calculated using a Student's unpaired t test or ANOVA with Tukey post hoc test for groups of three or more. *$p < 0.05$, **$p < 0.01$, ***$p < 0.001$.

iNKT-deficient mice (*CD1d*$^{-/-}$) (Figures S3E and S3F). CLAMS studies revealed that *CD1d*$^{-/-}$ mice had a lower metabolic rate than WT mice (Figures S4A and S4B), consistent with the increase in adiposity previously described (Lynch et al., 2012). Liraglutide induced a slight decrease in overall VO_2 and VCO_2 in both WT and *CD1d*$^{-/-}$ mice (Figures S4A and S4B), in

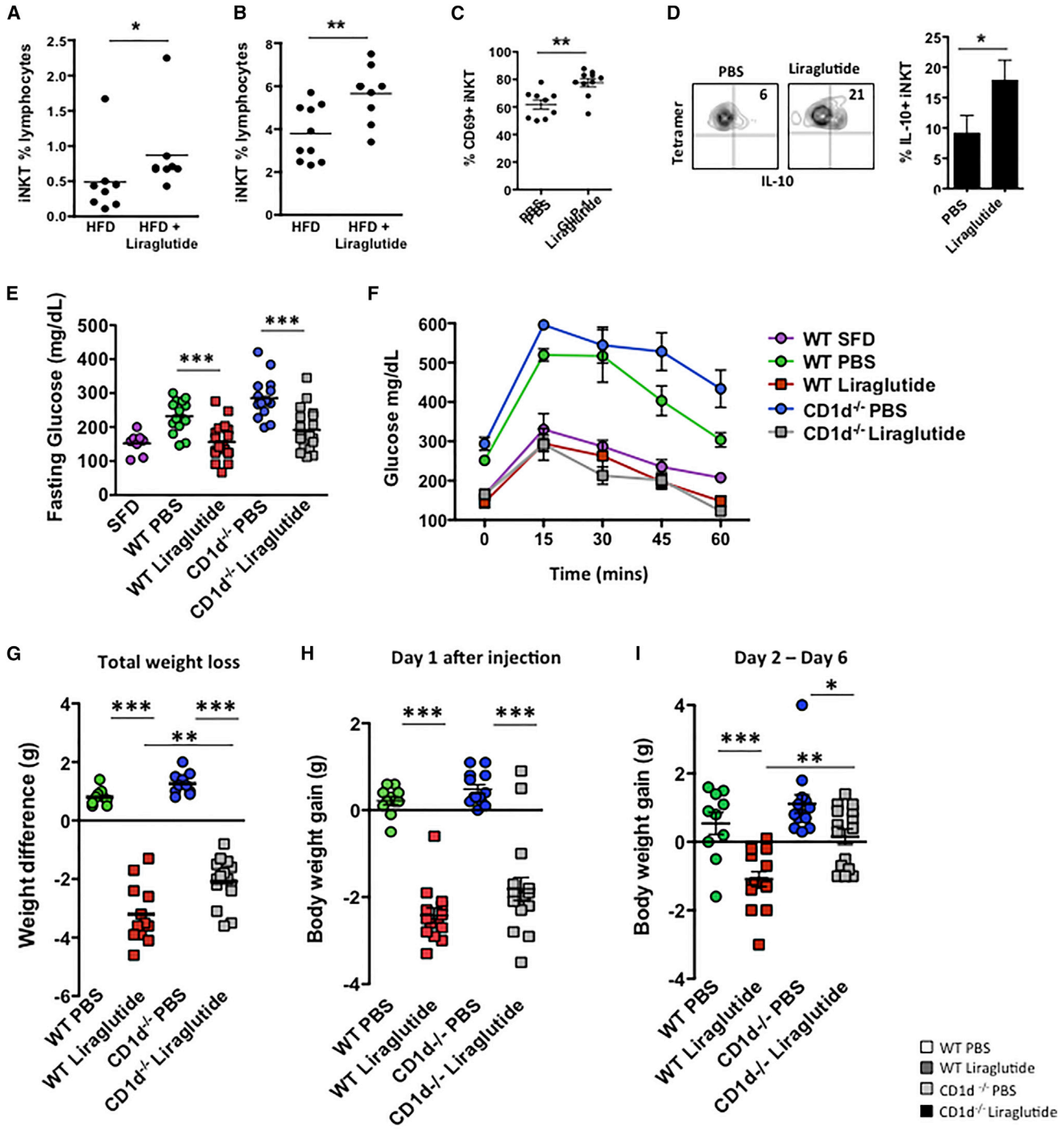

(legend on next page)

agreement with reports that liraglutide-induced weight loss mainly reflects reduced appetite and energy intake (Harder et al., 2004; O'Shea et al., 1996; van Can et al., 2014). Nevertheless, central GLP-1R signaling can also induce thermogenesis through activation of BAT, which may account for a small proportion of liraglutide weight loss effects (Lockie et al., 2012). Thus, we investigated if i.p. liraglutide treatment induced browning of white inguinal fat. Liraglutide induced a robust thermogenic gene expression program in WT mice, including upregulation of UCP-1, PGC1α, and Cidea (Figure 3J). Importantly, this response was blunted or lost in *CD1d*$^{-/-}$ mice (Figure 3J). Liraglutide administered intraperitoneally did not induce a significant change in thermogenic genes in BAT, although a trend was seen in WT, but not *CD1d*$^{-/-}$, mice (Figure S4C). Together, our findings show (1) liraglutide activates iNKT cells, (2) iNKT cells are required for the thermogenic program in WAT induced by liraglutide, and (3) iNKT activation induces FGF21. Previous reports have linked GLP-1 analogs with increased FGF21 expression (Nonogaki et al., 2014; Yang et al., 2012). Thus, we examined whether iNKT cells were required for the induction of FGF21 by liraglutide. Liraglutide robustly induced FGF21 expression in WT inguinal adipose tissue; however, FGF21 was not induced in mice lacking iNKT cells (Figure 3K). Liraglutide also induced expression of FGF21 receptors FGFR and β-klotho in adipose tissue of WT, but not in *CD1d*$^{-/-}$, mice (Figure 3L). Adiponectin, a downstream regulator of FGF21 signaling, was also robustly induced in adipose tissue by liraglutide in WT, but not iNKT, cell-deficient mice (Figure 3M). Thus, although the primary mechanism of action for the weight loss effects of liraglutide is a reduction of energy intake, liraglutide also induces adiponectin, FGF21, and an adipose thermogenic program that requires a functional iNKT cell system.

Previously, we have shown that liraglutide can activate human iNKT cells in vitro (Hogan et al., 2011) and can increase levels of circulating adiponectin in obese individuals with type 2 diabetes (Hogan et al., 2014). To ascertain the existence of a GLP-1-iNKT cell-FGF21 axis in humans, we studied a cohort of nine newly diagnosed obese type 2 diabetes patients before and after 8 weeks of liraglutide therapy. HbA1c and body weight were reduced following liraglutide administration (Figures 4A and 4B). This was paired with a significant expansion in peripheral iNKT cell levels (Figure 4C). Liraglutide also significantly elevated circulating FGF21 levels (Figure 4D), which strongly correlated with the extent of weight loss: two individuals without weight loss did not display increases in FGF21, and the individuals who lost the most weight had the largest increases in FGF21 (Figure 4E). These data demonstrate that liraglutide expands iNKT cell number and increases FGF21 levels in obese humans, consistent with our findings in high-fat-fed mice.

Our data provide a mechanism whereby iNKT cells, by adoptive transfer or activation with their specific ligand αGalCer, induce rapid and robust weight loss. Our study shows that an innate T cell population, resident in adipose tissue, drives thermogenesis and weight loss. Thus, iNKT cells join the list of other immune cells that have been reported to control weight, namely ILC2s (Brestoff et al., 2015; Lee et al., 2015) and macrophages (Nguyen et al., 2011). iNKT cell actions are distinct from those previously published. ILC2 cell production of methionine-enkephalin peptides drove UCP1 expression and thermogenesis in WAT (Brestoff et al., 2015), while macrophages can produce catecholamines to sustain thermogenesis in cold temperatures (Nguyen et al., 2011). Here we show that iNKT activation drives production of FGF21 by adipocytes in WAT and a robust and sustained reduction in RER, indicating β-oxidation, coupled with UCP-1 expression, leading to thermogenic weight loss without affecting appetite. We also show that this pathway plays a role in another setting: liraglutide-induced weight loss. Although this pathway is not the main mechanism of liraglutide action, which is primarily satiety, our results highlight a role for activation of this iNKT-FGF21 pathway in the maximal weight loss effects of liraglutide in mice. Of additional relevance, the actions of liraglutide to induce FGF-21 and adiponectin also required a functional iNKT cell axis. Unlike other pathways of cytokine-driven activation of immune cells, iNKT cells can be specifically targeted in the clinic by αGalCer and related lipid ligand administration. αGalCer has been given to patients in several different clinical trials for cancer and has been proven safe and capable of activating human iNKT cells in vivo, with minimal side effects. This study suggests that targeting iNKT cells with specific ligands could represent a new therapeutic approach for subjects with metabolic disorders, such as non-alcoholic fatty liver disease or insulin resistance, that are sensitive to the actions of metabolic mediators such as adiponectin and FGF-21.

EXPERIMENTAL PROCEDURES

Patients

Details of patient collection are in the Supplemental Experimental Procedures. Blood was collected from ten type 2 diabetes patients before and after 8 weeks of GLP-1 analog therapy (0.6 mg once daily for 2 weeks, then 1.2 mg once daily

Figure 3. GLP-1 Analog Liraglutide Activates iNKT Cells In Vivo and In Vitro

WT mice fed an HFD for 6–8 weeks, then injected daily with GLP-1 analog liraglutide (50 μg/kg intraperitoneally) for 5 days (n = 5 per treatment per experiment; experiment performed four times).

(A and B) (A) Circulating peripheral and (B) adipose iNKT cells levels in obese mice after liraglutide treatment in vivo (n = 8–9 per group).

(C and D) (C) Graph of activation marker CD69 and (D) intracellular cytokine staining of IL-10 on adipose iNKT cells from obese WT mice post-PBS or liraglutide treatment (n = 9 per group).

(E–G) HFD-fed WT and *CD1d*$^{-/-}$ (no iNKT) mice were injected daily with GLP-1 analog liraglutide (50 μg/kg intraperitoneally) for 5 days and (E) fasting glucose and (F) glucose tolerance tests and (G) total weight loss in grams (g) were measured.

(H and I) (H) Weight loss after 24 hr, and (I) from 24 hr and 120 hr after liraglutide treatment.

In (E)–(I), n = 10 per group receiving PBS, and n = 13–14 per group receiving liraglutide.

(J–M) Graphs of transcripts for (J) UCP-1, Cidea, and PGC1α; (K) FGF21; (L) FGFR and β-klotho (KLB); and (M) adiponectin in inguinal adipose tissue of obese WT and *CD1d*$^{-/-}$ mice that received PBS or liraglutide for 5 days. n = 3 per group per experiment, repeated three times. Graphs show the mean (± SEM).

Statistics have been calculated using a Student's unpaired t test or ANOVA with Tukey post hoc test for groups of three or more. *$p < 0.05$, **$p < 0.01$, ***$p < 0.001$.

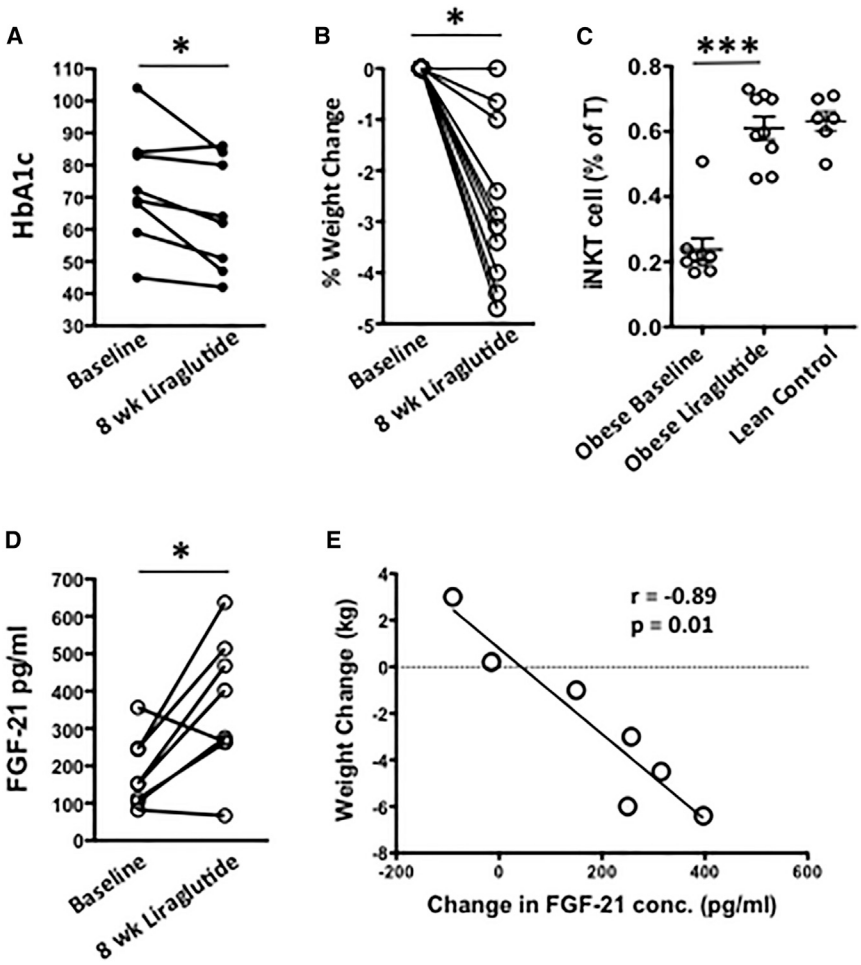

Figure 4. Liraglutide Activates Human iNKT Cells In Vivo and Induces FGF21

Obese patients with newly diagnosed type 2 diabetes received daily injections of liraglutide for 8 weeks, and peripheral blood was collected before and after.

(A–C) Change in (A) HbA1c (n = 8) and (B) body weight (n = 10) and (C) circulating iNKT cell levels in obese patients after 8 weeks of liraglutide therapy, with age-matched lean controls for comparison (n = 6).

(D and E) (D) Serum FGF21 concentration and (E) correlation between weight loss and change in FGF21 concentration in patients, before and after 8 weeks of liraglutide therapy. Each symbol represents one individual.

Statistical comparisons using Mann-Whitney U test and paired t tests. *$p < 0.05$, **$p \leq 0.01$.

by i.p. injection), and metabolic status, iNKT, and FGF21 levels were measured. Informed consent was obtained from all participants, and approval to conduct this study was obtained from the St. Vincent's Healthcare Group Ethics and Medical Research Committee.

Mice

Details of mouse strains are in the Supplemental Experimental Procedures. C57BL/6 mice were purchased from Jackson Laboratory. *CD1d*$^{-/-}$ and *Ja18*$^{-/-}$ were provided by Mark Exley (Harvard). FGF21 null mice were kindly provided by Eli Lily (Badman et al., 2009). All animal work was approved by and in compliance with the Institutional Animal Care and Use Committee guidelines of the Dana Farber Cancer Institute and Harvard Medical School.

Mouse Manipulations

Details of cell isolation and flow cytometry can be found in the Supplemental Experimental Procedures. iNKT cells were measured using αGalCer analog PBS-57-loaded or empty CD1d tetramers provided by the NIH tetramer facility. For in vivo treatment, mice were injected intraperitoneally with a single injection of αGalCer or vehicle in 150 μL volume. For liraglutide treatment, mice received daily injection of GLP-1 analog (50 μg/kg intraperitoneally) for 5 days. For CLAMS analysis, mice were singly housed and acclimated, then administered vehicle control, monitored for 70 hr, given 1 μg αGalCer in 150 μL intraperitoneally, and monitored for a further 70 hr.

Statistics

The changes of outcomes between baseline and the follow-up were evaluated using paired t tests. The difference between treatment groups was tested using unpaired two-sample t tests with Welsh's correction for unequal variances and one-way ANOVA followed by Tukey's post hoc test. $p \leq 0.05$ was considered significant.

SUPPLEMENTAL INFORMATION

Supplemental Information includes Supplemental Experimental Procedures and four figures and can be found with this article online at http://dx.doi.org/10.1016/j.cmet.2016.08.003.

AUTHOR CONTRIBUTIONS

L.L. designed and performed experiments and analyzed data; A.E.H. and D.O.S. designed and performed the human work. D.D., C.L., A.G., M.C., D.S., and K.L. performed experiments; A.B., M.B., D.E.C., E.M.-F., and D.J.D. contributed to the design of experiments and provided materials and tools; B.L. performed statistical analysis; and L.L., D.J.D., and M.B. wrote the paper.

ACKNOWLEDGMENTS

The authors would like to thank Eli Lily for the use of *FGF21*$^{-/-}$ mice and the NIH Tetramer Core for mouse CD1d-PBS57 tetramers. L.L. was supported by an American Diabetes JF Development Award (116JDF061), a BWH Evergreen Innovation Grant, a BADERC grant, and an ERC Stg grant (679173); M.B. is supported by research grants from the NIH (AI063428 and AI028973); and A.H. and D.O.S. are supported by the Health Research Board Ireland. M.B. is supported by NIHR01 111144. D.J.D. is supported by the Canada Research

Chairs program, CIHR grant 123391, and a BBDC-Novo Nordisk Chair in diabetes research. D.O.S. and M.B. contributed equally to this paper.

Received: May 12, 2015
Revised: January 5, 2016
Accepted: August 3, 2016
Published: September 1, 2016

REFERENCES

Badman, M.K., Koester, A., Flier, J.S., Kharitonenkov, A., and Maratos-Flier, E. (2009). Fibroblast growth factor 21-deficient mice demonstrate impaired adaptation to ketosis. Endocrinology *150*, 4931–4940.

Baggio, L.L., and Drucker, D.J. (2007). Biology of incretins: GLP-1 and GIP. Gastroenterology *132*, 2131–2157.

Brestoff, J.R., Kim, B.S., Saenz, S.A., Stine, R.R., Monticelli, L.A., Sonnenberg, G.F., Thome, J.J., Farber, D.L., Lutfy, K., Seale, P., and Artis, D. (2015). Group 2 innate lymphoid cells promote beiging of white adipose tissue and limit obesity. Nature *519*, 242–246.

Brigl, M., and Brenner, M.B. (2004). CD1: antigen presentation and T cell function. Annu. Rev. Immunol. *22*, 817–890.

Cousin, B., Cinti, S., Morroni, M., Raimbault, S., Ricquier, D., Pénicaud, L., and Casteilla, L. (1992). Occurrence of brown adipocytes in rat white adipose tissue: molecular and morphological characterization. J. Cell Sci. *103*, 931–942.

Enerbäck, S. (2009). The origins of brown adipose tissue. N. Engl. J. Med. *360*, 2021–2023.

Enerbäck, S., Jacobsson, A., Simpson, E.M., Guerra, C., Yamashita, H., Harper, M.E., and Kozak, L.P. (1997). Mice lacking mitochondrial uncoupling protein are cold-sensitive but not obese. Nature *387*, 90–94.

Fisher, F.M., Kleiner, S., Douris, N., Fox, E.C., Mepani, R.J., Verdeguer, F., Wu, J., Kharitonenkov, A., Flier, J.S., Maratos-Flier, E., and Spiegelman, B.M. (2012). FGF21 regulates PGC-1α and browning of white adipose tissues in adaptive thermogenesis. Genes Dev. *26*, 271–281.

Gaich, G., Chien, J.Y., Fu, H., Glass, L.C., Deeg, M.A., Holland, W.L., Kharitonenkov, A., Bumol, T., Schilske, H.K., and Moller, D.E. (2013). The effects of LY2405319, an FGF21 analog, in obese human subjects with type 2 diabetes. Cell Metab. *18*, 333–340.

Hadjiyanni, I., Siminovitch, K.A., Danska, J.S., and Drucker, D.J. (2010). Glucagon-like peptide-1 receptor signalling selectively regulates murine lymphocyte proliferation and maintenance of peripheral regulatory T cells. Diabetologia *53*, 730–740.

Hams, E., Locksley, R.M., McKenzie, A.N., and Fallon, P.G. (2013). Cutting edge: IL-25 elicits innate lymphoid type 2 and type II NKT cells that regulate obesity in mice. J. Immunol. *191*, 5349–5353.

Hanssen, M.J., Broeders, E., Samms, R.J., Vosselman, M.J., van der Lans, A.A., Cheng, C.C., Adams, A.C., van Marken Lichtenbelt, W.D., and Schrauwen, P. (2015). Serum FGF21 levels are associated with brown adipose tissue activity in humans. Sci. Rep. *5*, 10275.

Harder, H., Nielsen, L., Tu, D.T., and Astrup, A. (2004). The effect of liraglutide, a long-acting glucagon-like peptide 1 derivative, on glycemic control, body composition, and 24-h energy expenditure in patients with type 2 diabetes. Diabetes Care *27*, 1915–1921.

Himms-Hagen, J., Cui, J., Danforth, E., Jr., Taatjes, D.J., Lang, S.S., Waters, B.L., and Claus, T.H. (1994). Effect of CL-316,243, a thermogenic beta 3-agonist, on energy balance and brown and white adipose tissues in rats. Am. J. Physiol. *266*, R1371–R1382.

Hogan, A.E., Tobin, A.M., Ahern, T., Corrigan, M.A., Gaoatswe, G., Jackson, R., O'Reilly, V., Lynch, L., Doherty, D.G., Moynagh, P.N., et al. (2011). Glucagon-like peptide-1 (GLP-1) and the regulation of human invariant natural killer T cells: lessons from obesity, diabetes and psoriasis. Diabetologia *54*, 2745–2754.

Hogan, A.E., Gaoatswe, G., Lynch, L., Corrigan, M.A., Woods, C., O'Connell, J., and O'Shea, D. (2014). Glucagon-like peptide 1 analogue therapy directly modulates innate immune-mediated inflammation in individuals with type 2 diabetes mellitus. Diabetologia *57*, 781–784.

Holland, W.L., Adams, A.C., Brozinick, J.T., Bui, H.H., Miyauchi, Y., Kusminski, C.M., Bauer, S.M., Wade, M., Singhal, E., Cheng, C.C., et al. (2013). An FGF21-adiponectin-ceramide axis controls energy expenditure and insulin action in mice. Cell Metab. *17*, 790–797.

Huh, J.Y., Kim, J.I., Park, Y.J., Hwang, I.J., Lee, Y.S., Sohn, J.H., Lee, S.K., Alfadda, A.A., Kim, S.S., Choi, S.H., et al. (2013). A novel function of adipocytes in lipid antigen presentation to iNKT cells. Mol. Cell. Biol. *33*, 328–339.

Ji, Y., Sun, S., Xia, S., Yang, L., Li, X., and Qi, L. (2012). Short term high fat diet challenge promotes alternative macrophage polarization in adipose tissue via natural killer T cells and interleukin-4. J. Biol. Chem. *287*, 24378–24386.

Kharitonenkov, A., and Adams, A.C. (2013). Inventing new medicines: the FGF21 story. Mol. Metab. *3*, 221–229.

Kharitonenkov, A., Shiyanova, T.L., Koester, A., Ford, A.M., Micanovic, R., Galbreath, E.J., Sandusky, G.E., Hammond, L.J., Moyers, J.S., Owens, R.A., et al. (2005). FGF-21 as a novel metabolic regulator. J. Clin. Invest. *115*, 1627–1635.

Lee, M.W., Odegaard, J.I., Mukundan, L., Qiu, Y., Molofsky, A.B., Nussbaum, J.C., Yun, K., Locksley, R.M., and Chawla, A. (2015). Activated type 2 innate lymphoid cells regulate beige fat biogenesis. Cell *160*, 74–87.

Lockie, S.H., Heppner, K.M., Chaudhary, N., Chabenne, J.R., Morgan, D.A., Veyrat-Durebex, C., Ananthakrishnan, G., Rohner-Jeanrenaud, F., Drucker, D.J., DiMarchi, R., et al. (2012). Direct control of brown adipose tissue thermogenesis by central nervous system glucagon-like peptide-1 receptor signaling. Diabetes *61*, 2753–2762.

Lovshin, J.A., and Drucker, D.J. (2009). Incretin-based therapies for type 2 diabetes mellitus. Nat. Rev. Endocrinol. *5*, 262–269.

Lynch, L., O'Shea, D., Winter, D.C., Geoghegan, J., Doherty, D.G., and O'Farrelly, C. (2009). Invariant NKT cells and CD1d(+) cells amass in human omentum and are depleted in patients with cancer and obesity. Eur. J. Immunol. *39*, 1893–1901.

Lynch, L., Nowak, M., Varghese, B., Clark, J., Hogan, A.E., Toxavidis, V., Balk, S.P., O'Shea, D., O'Farrelly, C., and Exley, M.A. (2012). Adipose tissue invariant NKT cells protect against diet-induced obesity and metabolic disorder through regulatory cytokine production. Immunity *37*, 574–587.

Lynch, L., Michelet, X., Zhang, S., Brennan, P.J., Moseman, A., Lester, C., Besra, G., Vomhof-Dekrey, E.E., Tighe, M., Koay, H.F., et al. (2015). Regulatory iNKT cells lack expression of the transcription factor PLZF and control the homeostasis of T(reg) cells and macrophages in adipose tissue. Nat. Immunol. *16*, 85–95.

Molofsky, A.B., Nussbaum, J.C., Liang, H.E., Van Dyken, S.J., Cheng, L.E., Mohapatra, A., Chawla, A., and Locksley, R.M. (2013). Innate lymphoid type 2 cells sustain visceral adipose tissue eosinophils and alternatively activated macrophages. J. Exp. Med. *210*, 535–549.

Nguyen, K.D., Qiu, Y., Cui, X., Goh, Y.P., Mwangi, J., David, T., Mukundan, L., Brombacher, F., Locksley, R.M., and Chawla, A. (2011). Alternatively activated macrophages produce catecholamines to sustain adaptive thermogenesis. Nature *480*, 104–108.

Nonogaki, K., Hazama, M., and Satoh, N. (2014). Liraglutide suppresses obesity and hyperglycemia associated with increases in hepatic fibroblast growth factor 21 production in KKAy mice. BioMed Res. Int. *2014*, 751930.

O'Shea, D., Gunn, I., Chen, X., Bloom, S., and Herbert, J. (1996). A role for central glucagon-like peptide-1 in temperature regulation. Neuroreport *7*, 830–832.

Qiu, Y., Nguyen, K.D., Odegaard, J.I., Cui, X., Tian, X., Locksley, R.M., Palmiter, R.D., and Chawla, A. (2014). Eosinophils and type 2 cytokine signaling in macrophages orchestrate development of functional beige fat. Cell *157*, 1292–1308.

Samms, R.J., Smith, D.P., Cheng, C.C., Antonellis, P.P., Perfield, J.W., 2nd, Kharitonenkov, A., Gimeno, R.E., and Adams, A.C. (2015). Discrete aspects of FGF21 in vivo pharmacology do not require UCP1. Cell Rep. *11*, 991–999.

Schipper, H.S., Rakhshandehroo, M., van de Graaf, S.F., Venken, K., Koppen, A., Stienstra, R., Prop, S., Meerding, J., Hamers, N., Besra, G., et al. (2012). Natural killer T cells in adipose tissue prevent insulin resistance. J. Clin. Invest. *122*, 3343–3354.

Turton, M.D., O'Shea, D., Gunn, I., Beak, S.A., Edwards, C.M., Meeran, K., Choi, S.J., Taylor, G.M., Heath, M.M., Lambert, P.D., et al. (1996). A role for glucagon-like peptide-1 in the central regulation of feeding. Nature *379*, 69–72.

van Can, J., Sloth, B., Jensen, C.B., Flint, A., Blaak, E.E., and Saris, W.H. (2014). Effects of the once-daily GLP-1 analog liraglutide on gastric emptying, glycemic parameters, appetite and energy metabolism in obese, non-diabetic adults. Int. J. Obes. *38*, 784–793.

Wang, Y.C., McPherson, K., Marsh, T., Gortmaker, S.L., and Brown, M. (2011). Health and economic burden of the projected obesity trends in the USA and the UK. Lancet *378*, 815–825.

Yang, M., Zhang, L., Wang, C., Liu, H., Boden, G., Yang, G., and Li, L. (2012). Liraglutide increases FGF-21 activity and insulin sensitivity in high fat diet and adiponectin knockdown induced insulin resistance. PLoS ONE *7*, e48392.

Cell Metabolism, Volume *24*

Supplemental Information

iNKT Cells Induce FGF21 for Thermogenesis and Are Required for Maximal Weight Loss in GLP1 Therapy

Lydia Lynch, Andrew E. Hogan, Danielle Duquette, Chantel Lester, Alexander Banks, Katherine LeClair, David E. Cohen, Abhisek Ghosh, Bing Lu, Michelle Corrigan, Darko Stevanovic, Eleftheria Maratos-Flier, Daniel J. Drucker, Donal O'Shea, and Michael Brenner

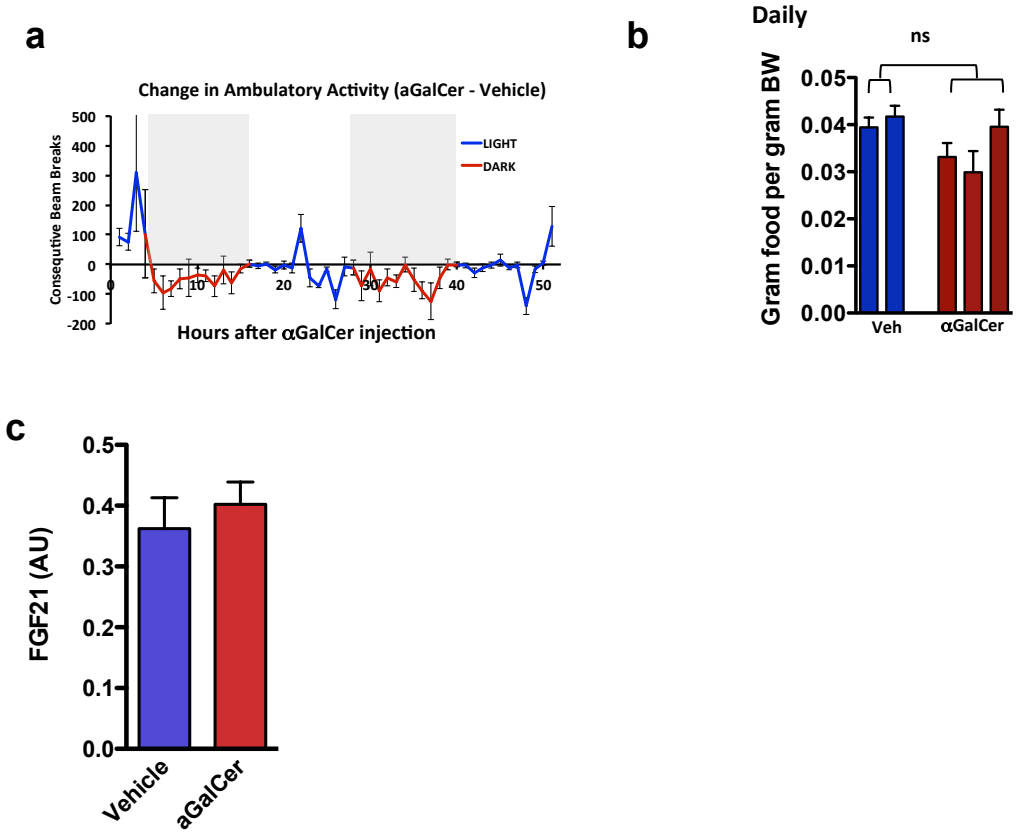

Figure S1, related to Figure 1: CLAMS analysis measuring movement and food intake of obese WT mice following aGalCer injection

A) Change in ambulatory movement obese WT mice after receiving αGalCer compared to vehicle i.p. Grey bars indicate dark periods B) Daily food intake in WT obese after receiving αGalCer or vehicle i.p. C) qPCR of FGF21 transcript in liver of obese WT mice treated with one injection of aGalCer or vehicle control.

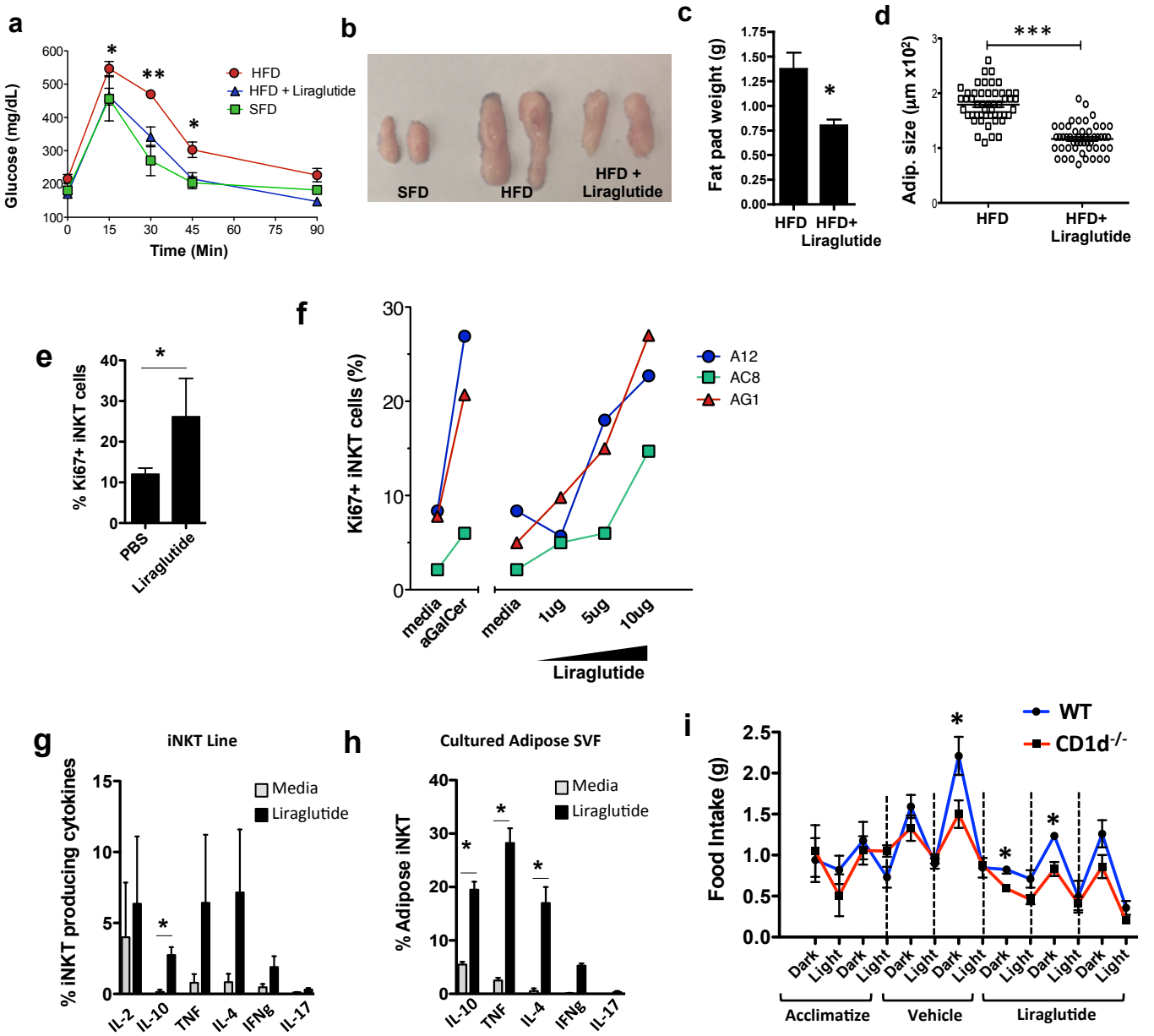

Figure S2, related to Figure 3: Liraglutide induces metabolic improvements and activates iNKT cells

A) Glucose tolerance test in WT mice on SFD or HFD receiving a daily injection of Liraglutide. Epididymal fat pad image (B) and weight (C) and adipocyte size (D) of WT mice on SFD or HFD 5 days after receiving a daily injection of Liraglutide or PBS. E) Liraglutide injection induces proliferation of iNKT cells in vivo as measured by Ki67 gated on CD1d-tetramer positive cells. F) Liraglutide activated iNKT cells directly in vitro. 3 primary cultured iNKT cell lines (A12, AC8 and AG1) were incubated *in vitro* with several doses of liraglutide for 18 hrs, or with aGalCer as a positive control for iNKT cell activation and proliferation. Intranuclear Ki67 staining was performed to measure iNKT cell proliferation. G) Intracellular staining for cytokines in iNKT cell lines (G) or adipose iNKT cells (H) cultured with or without liraglutide. I) Liraglutide induces significant decreases in food intake in both WT and CD1d-/- mice. Food intake in obese WT (blue) and CD1d$^{-/-}$ (red) mice during periods of acclimatization, control PBS injection and liraglutide injection. Grey bars indicate dark periods. Graphs show the mean (± s.e.m). Statistics have been calculated using a Student unpaired t-test or ANOVA with Tukey post-hoc test for groups of 3 or more. *$p < 0.05$, **$p < 0.01$, ***$p < 0.001$.

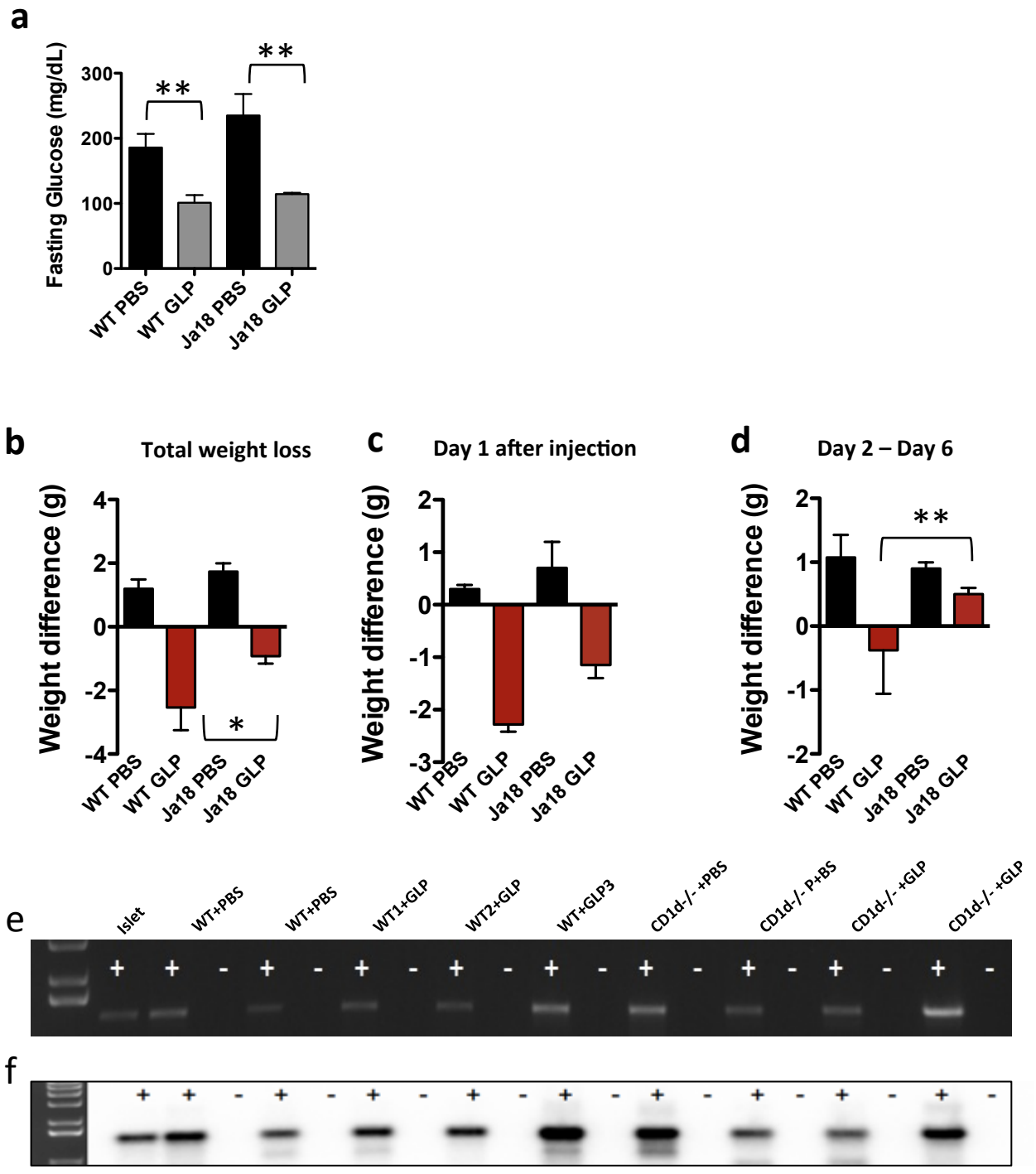

Figure S3, related to Figure 3: Differential effect of liraglutide on WT versus Ja18$^{-/-}$ mice
A) Fasting glucose levels in obese WT and Ja18$^{-/-}$ mice after treatment with liraglutide or PBS control for 5 days. B) Total weight loss in grams (g) after 5 days of Liraglutide treatment compared to PBS. C) Weight loss after 24hrs, and D) between 24 hours and 120hrs of Liraglutide treatment. E) PCR products using mGLP1R (1.338kb) primers on islets as a positive control, and hypothalmii from wt and CD1d$^{-/-}$ mice after i.p. injection with PBS or Liraglutide. RT+ = reverse transcriptase positive, RT- = reverse transcriptase minus. F) Southern blot of PCR products.

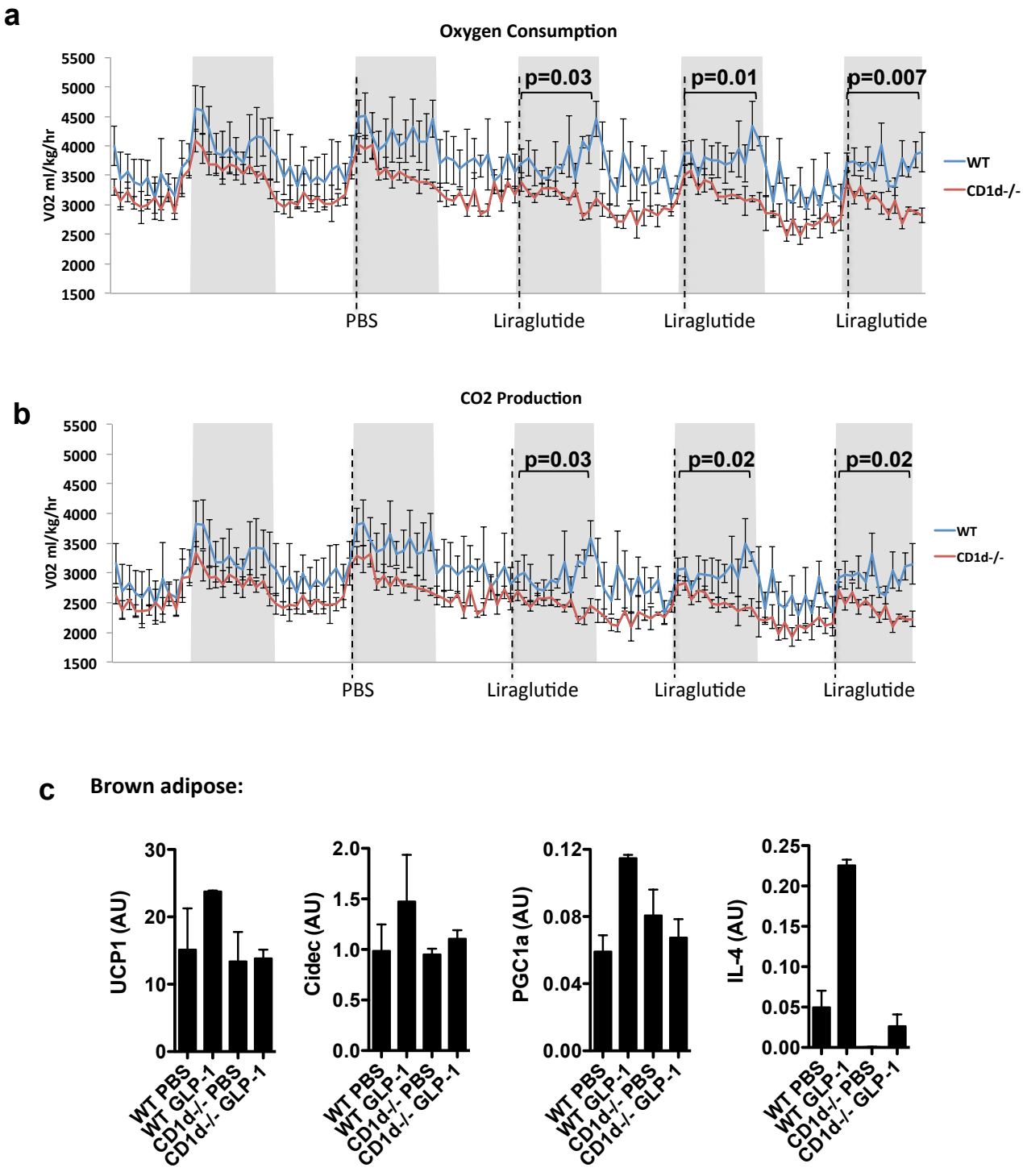

Figure S4, related to Figure 3: CLAMS analysis and BAT qPCR of obese WT and CD1d$^{-/-}$ mice on liraglutide treatment A) VO_2 and B) CO_2 in obese WT and CD1d$^{-/-}$ mice after PBS or liraglutide injection. C) RNA transcript levels (arbitrary units) of UCP1, Cidea, PGC1a and IL-4 in brown adipose tissue (BAT) from obese WT and CD1d-/- mice after treatment with PBS control or liraglutide for 5 days.

Supplemental Materials and Methods

GLP1 analog treatment

Patients: Ten participants with type 2 diabetes who were starting therapy the GLP-1 analogue in line with good clinical practice were enrolled. Each self-administered liraglutide, by subcutaneous injection, at a dose of 0.6mg once daily for two weeks and then 1.2mg once daily. Before and after 8 weeks of therapy the research participants attended for a visit in the early morning after an overnight fast. At this visit reported adherence to treatment was assessed, weight recorded and sample of blood was taken. The sampled blood was used to determine metabolic status and to assess peripheral iNKT levels. Informed consent was obtained from all participants and approval to conduct this study was obtained from the St Vincent's Healthcare Group Ethics and Medical Research Committee.

Mice: C57BL/6, mice were purchased from Jackson Laboratory. $CD1d^{-/-}$ and $Ja18^{-/-}$ were provided by Mark Exley (Harvard Medical School). FGF21-null mice were kindly provided by Eli Lily. FGF21-null mice were generated as previously reported (Badman et al., 2009). For targeted disruption of the Fgf21 locus, a 6.5-kb NheI genomic fragment containing all three exons of the mouse FGF21 gene was subcloned and used as a gene targeting vector by replacing part of exon 1 (30 bp downstream of the ATG), all of exon 2, and the 5′ region of exon 3 with a neomycin resistance gene (pGTN29; New England Biolabs, Ipswich, MA) thus deleting approximately 1200 bp of the genomic FGF21 sequence and deleting the 3′ part of exon 1, all of exon 2, and the 5′ region of exon 3. Founder mice were subsequently backcrossed onto the C57/BL6 line at least 10 times before investigation. In almost all experiments, male mice were used, with the exception of liraglutide treatments in WT and $CD1d^{-/-}$ where male and female mice were used and compared to male and female WT mice. Mice were bred in our specific-pathogen-free facilities at Harvard Medical School. All animal work was approved by and in compliance with the Institutional Animal Care and Use Committee guidelines of The Dana Farber Cancer Institute and Harvard Medical School.

Tissue processing

The visceral (epididymal), subcutaneous, peri-renal and brown adipose depots were isolated from the mice and digested with 20 mL collagenase solution (1mg/mL collagenase in PBS) at 37°C for 25 min with shaking. After digestion, adipocytes were isolated by filtering through a 40um nylon mesh and centrifuged for 5 min at 300g to pellet the stromovascular fraction (SVF). The supernatant was discarded and the SVF was washed with FACS buffer (1%FBS and 0.02% NaN3 in PBS), then resuspended in FC block at 4°C for 15 min and then stained with desired antibodies.

Flow cytometry

Single-cell suspensions were incubated with Fc receptor–blocking antibody before being stained on ice with specific antibodies and tetramer. Dead cells were excluded with live/dead gate using 7-AAD, or Zombie Aqua (BioLegend) for fixed and permeabilized cells. αGalCer analog PBS-57-loaded or empty CD1d tetramers were provided by the NIH tetramer facility (Emory Vaccine Center, Atlanta). For analysis of iNKT cells, a dump gate with CD19 was used to eliminate non-specific staining, and staining of the same cell preparations with 'empty' tetramer (no αGalCer) confirmed specificity. Antibodies conjugated to fluorescein isothiocyanate, phycoerythrin, phycoerythrin-indotricarbocyanine, peridinine chlorophyll protein complex 5.5, allphycocyanin or allophycocyanin-indotricarbocyanine were as follows: anti-IL-4 (11B11), -IFN-γ (XMG1,2), -IL-10 (JES5-16E3), -TCRβ (G572597). For staining for cytokines, cells were fixed and permeabilized with the Fix/Perm buffer set (eBioscience). Cell doublets were excluded by comparison of side-scatter width to forward-scatter area. For intracellular cytokine staining, single-cell suspension of adipose tissue SVFs were obtained as before, but with the inclusion of Brefeldin A in all media or *in vivo*. First, adipose SVF cells were stained with cell-surface-labelling CD3 mAb and αGalCer-loaded CD1d tetramer. Cells were then fixed, permeabilized, and stained intracellularly for Ki-67, IL-4, IL-10, and IFN-γ using the Cytofix/Cytoperm

kit (BD Biosciences), according to the manufacturer's instructions. For human iNKT cell identification, anti-human 6b11 antibody was used against anti-CD3, after gating on CD45+ cells that were negative for CD19 and CD14 (dump gate).

In Vivo treatment of mice, including stimulation of iNKT Cells

Mice were injected i.p. with a single injection of αGalCer or vehicle in 150 ul volume. Mice weighing between 25-42g received 1ug of αGalCer, and mice weighing more than 42g received 1ug of αGalCer. For liraglutide treatment, mice were fed a high fat diet and where randomly assigned to control or GLP-1 treated groups. Mice received daily injection of GLP-1 analogue (50ug/kg I.P) for 5 days. As a positive control for activation of brown adipose tissue through b-adrenergic stimulation, CL316,243 (Sigma-Aldrich) at 1 mg/kg was injected i.p.

CLAMS analysis

Wild type C57Bl/6 mice were maintained on a high fat diet before entering the comprehensive laboratory animal monitoring system (CLAMS). Each mouse served as its own control. The mice were singly housed and acclimated to the system for 48 hours then administered a vehicle control (150 ul PBS) by i.p. injection. These mice were further monitored for 70 hours before i.p. injection administration of 1μg αGalCer in 150 μl volume. These mice were monitored for 70 hours. Body weights were measured at the start and end of acclimation, vehicle injection and αGalCer injection. The CLAMS measures each parameter (oxygen consumption, CO_2 production, respiratory quotient, locomotor activity, food intake and body temperature) approximately every 10 minutes. For the data analysis, the measurements for each parameter were averaged over every hour for each mouse. For the αGalCer experiment, the data are presented based on the change in response of each mouse to the vehicle versus αGalCer treatment. These changes were averaged. To calculate change from vehicle by αGalCer injection the averages per hour of each mouse post vehicle injection were

subtracted from the averages per hour post αGalCer injection, so that the diurnal variation in measurements was maintained.

Thermal imaging of body temperature

Measurement of body temperature was performed using a thermal imaging camera (T300 InfraRed Camera; FLIR Systems). Tail temperature of obese WT mice 48 hours after αGalCer or vehicle treatment was analysed using FLIR Reporter 8.5 software (FLIR Systems). Images were acquired by anesthesizing mice and taking 2–3 images of each mouse from different angles were acquired to minimize temperature variations due to different postures of the animal. Software tools were used to point the region of interest at 1 cm and 2 cm down on the tail and average body temperature was calculated using area in each mouse.

Statistics

The continuous outcomes were expressed as the mean ± S.E.M. The changes of outcomes between baseline and the follow-up were evaluated using paired t tests. The difference between treatment groups were tested using unpaired two sample *t* tests with Welsh's correction for unequal variances and one-way analysis of variance (ANOVA) followed by Tukey's post-hoc test. $P \leq 0.05$ was considered to denote significance. No exclusion of data points or mice was used. Pilot studies were used for estimation of the sample size required to ensure adequate power. Mice that received treatment were randomized per cage so that each cage contained mice with test treatment versus control treatment (eg. αGalCer vs vehicle, or liraglutide vs. PBS).